DOI: 10.6060/ivkkt.20196207.5947

УДК: 537.525

ПАРАМЕТРЫ ПЛАЗМЫ И КИНЕТИКА АКТИВНЫХ ЧАСТИЦ В СМЕСИ HBr + Cl_2 + O_2

А.М. Ефремов, В.Б. Бетелин, К.Х. Квон, Д.Г. Снегирев

Александр Михайлович Ефремов*

Кафедра технологии приборов и материалов электронной техники, Ивановский государственный химико-технологический университет, Шереметевский пр., 7, Иваново, Российская Федерация, 153000
Кафедра естественнонаучных дисциплин, Ивановская пожарно-спасательная академия ГПС МЧС России, пр. Строителей, 33, Иваново, Российская Федерация, 153040
E-mail: efremov@isuct.ru*

Владимир Борисович Бетелин

Федеральный научный центр Научно-исследовательский институт системных исследований РАН, Нахимовский просп., 36, к.1, Москва, Российская Федерация, 117218

Кванг-Хо Квон

Лаборатория применения плазмы, Департамент разработки средств и методов контроля, Университет Корея, 208 Сеочанг-Донг, Чочивон, Республика Корея, 339-800

Дмитрий Геннадьевич Снегирев

Кафедра естественнонаучных дисциплин, Ивановская пожарно-спасательная академия ГПС МЧС России, пр. Строителей, 33, Иваново, Российская Федерация, 153040

В данной работе проведено комбинированное (экспериментальное и теоретическое) исследование характеристик газовой фазы индукционного 13,56 МГц ВЧ-разряда низкого давления в трехкомпонентной смеси HBr + Cl_2 + O_2. Данные по внутренним параметрам плазмы, кинетике плазмохимических процессов и стационарному составу газовой фазы были получены при совместном использовании диагностики плазмы зондами Ленгмюра и 0-мерной (глобальной) модели плазмы. Условия эксперимента и моделирования соответствовали постоянным значениям общего давления плазмообразующего газа (p = 10 мтор), вкладываемой мощности (W = 500 Вт), мощности смещения (W_{dc} = 200 Вт) и содержания кислорода в смеси (y(O_2) = 11 %). В качестве варьируемого параметра выступало соотношение начальных концентраций компонентов в паре HBr + Cl_2, которое изменялось в диапазоне 0 – 89 % Cl_2. Было найдено, что замещение HBr на Cl_2 в исследуемом диапазоне условий: 1) приводит к увеличению средней энергии и концентрации электронов; 2) вызывает немонотонное (с максимумом при ~ 45 % Cl_2) изменение концентрации атомов Br; и 3) обеспечивает рост концентрации атомов O в условиях y(O_2) = const. На основе расчетных данных по плотностям потоков активных частиц (атомов Br, Cl и O, положительных ионов) проведен анализ возможных механизмов влияния соотношения начальных концентраций в паре HBr + Cl_2 на кинетику травления Si и SiO_2.

Ключевые слова: параметры плазмы, скорость реакции, поток атомов галогенов, поток энергии ионов, скорости травления Si и SiO_2

PLASMA PARAMETERS AND KINETICS OF ACTIVE SPECIES IN HBr + Cl_2 + O_2 GAS MIXTURE

A.M. Efremov, V.B. Betelin, K.-H. Kwon, D.G. Snegirev

Aleksandr M. Efremov*

Department of Electronic Devices and Materials Technology, Ivanovo State University of Chemistry and Technology, Sheremetevskiy av., 7, Ivanovo, 153000, Russia
Department of Natural Science Courses, Ivanovo Firefighting and Rescues Academy, Stroiteley av., 33, Ivanovo, 153040, Russia
E-mail: efremov@isuct.ru*

Vladimir B. Betelin

Scientific Research Institute of System Development RAS, Nakhimovsky ave., 36, bld. 1, Moscow 117218, Russia

Kwang-Ho Kwon

Plasma Application Lab., Dept. of Instrumentation and Control Engineering, Korea University, 208 Seochang-Dong, Chochiwon, Korea, 339-800

Dmitriy G. Snegirev

Department of Natural Science Courses, Ivanovo Firefighting and Rescues Academy, Stroiteley av., 33, Ivanovo, 153040, Russia

In this work, we performed the combined (experimental and model-based) study of gas-phase plasma characteristics for HBr + Cl_2 + O_2 gas mixture under conditions of low-pressure inductive 13.56 MHz discharge. The data on internal plasma parameters, plasma chemistry as well as the steady-state plasma composition were obtained using a combination of Langmuir probe diagnostics and 0-dimensional (global) plasma modeling. Both experimental and modeling procedures were carried out at constant total gas pressure (p = 10 mTorr), input power (W = 500 W), bias power (W_{dc} = 200 W) and O_2 fraction in a feed gas ($y(O_2)$ = 11 %). The variable parameter was the HBr + Cl_2 mixing ratio, which was changed in the range of 0 – 89 % Cl_2. It was found that, under the given set of experimental conditions, the substitution of HBr for Cl_2: 1) results in increasing both mean electron energy and electron density; 2) causes the mon-monotonic (with a maximum at ~ 45 % Cl_2) change in Br atom density; and 3) provides an increase in O atom density at $y(O_2)$ = const. The possible impacts of HBr + Cl_2 mixing ratio on Si and SiO_2 etching kinetics were estimated through the analysis of model-predicted fluxes for plasma active species (Br, Cl and O atoms, positive ions).

Key words: plasma parameters, reaction rate, halogen atom flux, ion energy flux, Si and SiO_2 etching rates

Для цитирования:

Ефремов А.М., Бетелин В.Б., Квон К.Х., Снегирев Д.Г. Параметры плазмы и кинетика активных частиц в смеси HBr + Cl_2 + O_2. *Изв. вузов. Химия и хим. технология*. 2019. Т. 62. Вып. 7. С. 72–79

For citation:

Efremov A.M., Betelin V.B., Kwon K.-H., Snegirev D.G. Plasma parameters and kinetics of active species in HBr + Cl_2 + O_2 gas mixture. *Izv. Vyssh. Uchebn. Zaved. Khim. Khim. Tekhnol*. 2019. V. 62. N 7. P. 72–79

INTRODUCTION

Silicon and silicon dioxide have found numerous applications in modern electronic device technology [1-3]. Since most of the applications assume precision patterning of the material surface, the development of dry etching processes for these materials is an important task to be solved for achieving advanced device performance.

Until now, there were a large number of experimental and theoretical works dealt with etching characteristics for both Si and SiO_2 in fluorine-based gas chemistries [3–5]. Results of these works provide detailed data on relationships between processing conditions (pressure, input power, and bias power), internal plasma parameters and heterogeneous stages of the etching process. Particularly, it was found that the principal disadvantage of all fluorine-based gas chemistries is the spontaneous Si + F reaction that results in low etching anisotropy of both mono- and poly-silicon. The last problem may be solved by using chlorine- and bromine-based gas chemistries in a form of Cl_2- and HBr-containing gas mixtures [6]. There were several studies have reported on the plasma-assisted etching characteristics for Si and SiO_2 in HBr- and Cl_2-based chemistries, for example Refs. [6-12]. When summarizing published data, one should mention following principal issues:

1) The probability of spontaneous chemical reaction Si + Cl/Br at typical process temperatures is much lower than that for Si + F. This effect is normally attributed to bigger sizes of Cl/Br atoms that retard their penetration inside the lattice of etched material. Also, the spontaneous reaction SiO_2 + Cl/Br is thermodynamically forbidden. Accordingly, the steady-state etching of Si and SiO_2 in Cl- or Br-based chemistries requires ion bombardment in order to destruct the Si-O

bonds and/or sputter the low volatile non-saturated $SiCl_x$ and $SiBr_x$ compounds.

2) Etching rates of both Si and SiO_2 in HBr plasma are lower than those in Cl_2 plasma under one and the same processing conditions. This fact correlates with differences in volume densities and fluxes of halogen atoms in these gas systems. At the same time, the HBr plasma provides more anisotropies etching together with the better etching selectivity in respect to photoresist masks.

3) The addition of oxygen to HBr or Cl_2 results in more anisotropic etching of Si and SiO_2, but lowers the absolute etching rates for both materials. This effect is attributed to the formation of lower volatile SiO_xBr_y and SiO_xCl_y compounds that passivate the sidewalls.

Unfortunately, the most of mentioned works had the purely experimental nature and thus, did not analyze the relationships between gas-phase and heterogeneous chemistries. In addition, there are no studies which consider plasma chemistry and etching kinetics in the three-component $HBr+Cl_2+O_2$ gas mixture. At the same time, the $HBr+Cl_2+O_2$ gas system may exhibit the positive features of both bromine- and chlorine-based gas chemistries as well as provide some additional effects due to specific changes in plasma parameters and densities of plasma active species.

In this work, we combined the experimental and model-based approaches to analyze plasma chemistry in $HBr+Cl_2+O_2$ inductively coupled plasma. The main goals were 1) to determine how the HBr/Cl_2 mixing ratio influences gas-phase plasma characteristics (electron temperature, energy of ion bombardment, densities, and fluxes of plasma active species); and 2) to establish the gas-phase-related parameters applicable for the analysis of Si and SiO_2 etching mechanisms.

EXPERIMENTAL AND MODELING DETAILS

The experiments were performed in the planar inductively coupled plasma (ICP) reactor [13]. The reactor chamber had a cylindrical shape (r = 16 cm, l = 12.8 cm) and was made from anodized aluminum. Plasma was excited using a 13.56 MHz rf power supply connected to a flat copper coil on the top side of the reactor chamber while another 12.56 MHz RF power supply was used to produce the negative dc bias voltage ($-U_{dc}$) on the bottom electrode. The experiments were conducted at constant gas pressure (p = 10 mTorr), total gas flow rate (q = 45 sccm), input power (W = 500 W) and bias power (W_{dc} = 200 W). The initial content of each component in the $HBr+Cl_2+O_2$ gas mixture was adjusted through the corresponding partial flow rates. Particularly, the O_2 flow rate was always 5 sccm that corresponded to $y(O_2) = q(O_2)/q = 11\%$. Accordingly, the variation of $q(Cl_2)$ in the range of 0-40 sccm provided $y(Cl_2)$ = 0-89% as well as the full substitution of HBr for Cl.

Plasma parameters were measured by double Langmuir probe tool DLP2000 (Plasmart Inc). The treatment of I-V curves aimed at obtaining electron temperature (T_e) and ion saturated current density (j_+) was based on well-known statements of the double Langmuir probe theory [14, 15]. In order to analyze the chemistry of plasma active species, we developed a simplified zero-dimensional kinetic model with using the data of T_e and n_+ as input parameters [13, 16, 17]. The electron density (n_e) was extracted from the measured n_+ using the solution of the steady-state chemical kinetic equation for negative ions together with the quasi-neutrality equation [16, 17]. Dissociative attachment rate coefficients for dominant electronegative components were either directly taken from Refs. [16-18] or estimated using known process cross-sections [19]. The set of chemical reactions included in the model was taken from a series of published works devoted to the modeling of HBr+Ar [13, 20], Cl_2+Ar [18, 21], O_2+Ar [18, 22], Cl_2+O_2 [18, 23], and $HBr+Cl_2$ [16] plasmas. The given kinetic schemes (reaction sets with corresponding rate coefficients) have demonstrated an acceptable agreement between model-predicted and measured plasma parameters for HBr, Cl_2 and O_2 [18, 20, 21, 24]. Similarly, to Refs. [13, 16], the model used following assumptions: 1) the electron energy distribution function (EEDF) is close to Maxwellian one; 2) the heterogeneous chemistry of atoms and radicals can be described in terms of the conventional first-order recombination kinetics; and 3) The temperature of the neutral ground-state species (T_{gas}) is independent on the feed gas composition. Since the experimental data on gas temperature were not available in this study, we took T_{gas} = 600 K as the typical value for the ICP etching reactors with similar geometry under the close range of experimental conditions [10-12].

For the analysis of heterogeneous chemistry, the fluxes of neutral species with the volume density n were calculates as $\Gamma \approx 0.25 n \upsilon_T$, where υ_T is the thermal velocity corresponding to the given T_{gas} value. The total flux of positive ions was evaluated as $\Gamma_+ = j_+/e$. The ion bombardment energy was found as $\varepsilon_i = -e(U_{dc} + U_f)$, where U_{dc} is the negative dc bias on the bottom electrode provided by W_{dc}, and $U_f \approx 0.5 T_e \ln(m_e/2.3m_+)$ is the floating potential. The effective ion mass m_+ was determined using fractions of neutral components with accounting for the differences in corresponding ionization rates and ion transport coefficients.

RESULTS AND DISCUSSION

The principal features of plasma parameters and gas-phase kinetics in the two-component $HBr+Cl_2$ gas mixture have been discussed in our previous work [16]. Taking into account that the current work 1) deals with processing conditions which are very close to those used in Ref. [16]; and 2) studies the $HBr+Cl_2+O_2$ system with $y(O_2)$ = const, it would be reasonable to focus the main attention on the effects resulting from the presence of oxygen.

Fig. 1 illustrates the influence of feed gas composition on measured and model-predicted plasma parameters.

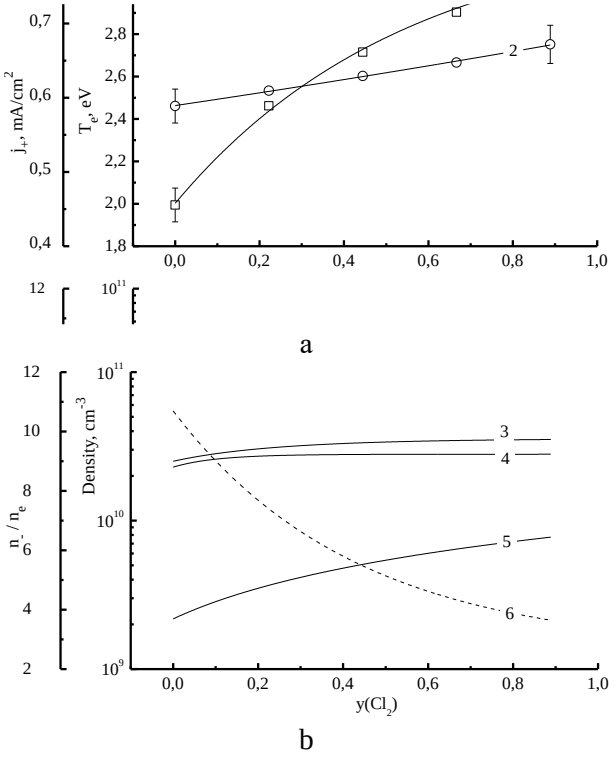

Fig. 1. Measured (1, 2) and model-predicted (3–6) plasma parameters as functions of Cl_2 fraction in a feed gas. In Fig. a): 1–electron temperature; 2–ion current density. In Fig. b): 3–total positive ion density; 4–total negative ion density; 5–electron density; 6–relative density of negative ions (n_-/n_e). The process condition are: $y(O_2)$ = 11 %, W = 500 W and W_{dc} = 200 W

Рис. 1. Экспериментальные (1, 2) и расчетные (3–6) параметры плазмы в зависимости от содержания Cl_2 в исходной смеси. На рис. а): 1–температура электронов; 2–плотность ионного тока. На рис. б): 3–суммарная концентрация положительных ионов; 4–суммарная концентрация отрицательных ионов; 5–концентрация электронов; 6–относительная концентрация отрицательных ионов (n_-/n_e). Условия процесса: $y(O_2)$ = 11 %, W = 500 Вт and W_{dc} = 200 Вт

An increase in $y(Cl_2)$ from 0-89% (in fact, the full substitution of HBr for Cl_2 in the $HBr + Cl_2 + 11\%$ O_2 gas mixture weak increase in T_e (2.5-2.8 eV, see Fig 1(a)) due to the decreasing electron energy loss in inelastic collisions with gas species. The reason is that the higher dissociation degree for Cl_2 molecules) causes a compared with HBr provides a higher fraction of atomic species in the Cl_2-rich plasmas. Accordingly, since Cl atoms are characterized by higher threshold energies and lower inelastic cross-sections (mainly for electronic excitation and ionization) compared with those for HBr, HCl and Br, the simultaneous increase in $y(Cl_2)$ and decrease in y(HBr) enriches EEDF by the high-energy electrons and shifts T_e toward higher values. Similar effects have been reported for many binary gas mixtures, including HBr+Ar, Cl_2+Ar and HBr+ Cl_2 plasmas [16, 20, 21]. A growth in both $n_+ = 2.5\times10^{10}$-3.5×10^{10} cm^{-3} and $n_e = 2.1\times10^9$-7.8×10^9 cm^{-3} (Fig. 1(b)) is the result of increasing total ionization frequency. This is due to the much higher ionization rate coefficient for Cl_2 molecules (~ 1.3×10^{-9} cm^3/s vs. ~ 6.7×10^{-10} cm^3/s for HBr and ~ 6.8×10^{-10} cm^3/s for Br at T_e = 3 eV) and an increase in all ionization rate coefficients together with increasing T_e (due to $\varepsilon_{iz} > 3/2T_e$, where ε_{iz} is the threshold energy for ionization). The behavior of the ion current density (j_+ = 0.5-0.8 mA/cm^2 for 0-89% Cl_2, see Fig. 1(a)) directly correlates with n_+. Finally, a decrease in the n_-/n_e ratio (10.7-3.5 for 0-89% Cl_2, see Fig. 1(b)) is the result of a nearly constant total negative ion density $n_- \approx 2.7\times10^{10}$ cm^{-3}. The last effect is due to the nearly proportional increase in both total attachment rate and ion-ion recombination frequency.

Fig. 2 shows the effect of $y(Cl_2)$ on the steady-state densities of neutral species. It was found that, under the given set of process conditions, pure HBr plasma keeps all the features of neutral species kinetics mentioned in previous works [13, 16, 20]. These are as follows: 1) reactions R1: HBr + e → H + Br + e (k_1 ~ 1.6×10^{-19} cm^3/s at T_e = 3 eV) and R2: Br_2 + e → 2Br + e (k_2 ~ 1.2×10^{-8} cm^3/s at T_e = 3 eV) represent the nearly equal sources of Br atoms; 2) the condition $k_2 >> k_3$ (where R3: H_2 + e → 2H + e) as well as the fast decay of H atoms through R4: HBr + H → H_2 + Br (k_4 ~ 1.2×10^{-11} cm^3/s) and R5: Br_2 + H → HBr + Br (k_5 ~ 1.2×10^{-10} cm^3/s) results in [Br] >> [H]; 3) high formation rates for H_2 in gas-phase process R4 and Br_2 in heterogeneous process R6: 2Br → Br_2 (k_6 ~ 125 s^{-1}) lead to $[H_2] \approx [Br_2] \approx$ [Br]; and 4) the effective recovery of the original HBr molecules through R5 provides the domination of this species over other neutral components.

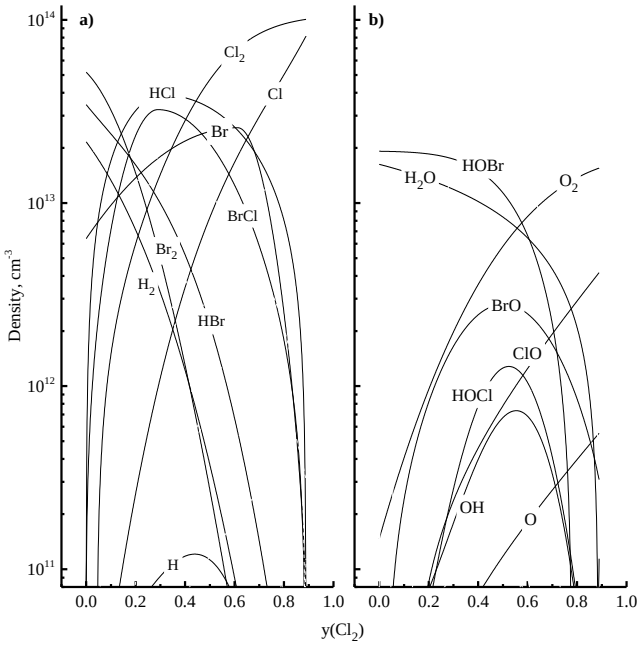

Fig. 2. Steady-state densities of oxygen-free (a) and oxygen-containing (b) neutral species as functions of Cl_2 fraction in a feed gas. The process conditions correspond to Fig. 1

Рис. 2. Стационарные концентрации бескислородных (а) и кислородсодержащих (б) нейтральных частиц в зависимости от содержания Cl_2 в исходной смеси. Условия процесса соответствуют рис. 1

The transition to the 89% HBr + 11% O_2 gas mixture lowers the Br atom formation rate in R1 + R2, but supplies several additional channels for the dissociation of HBr (R7–R9) and Br_2 (R10–R12) owing to their interactions with O, O(^{1}D), and OH:

$$HBr + O \rightarrow OH + Br \quad (k_7 \sim 3.6\times10^{-13}\ cm^3/s) \qquad (R7)$$

$$HBr + O(^1D) \rightarrow OH + Br \quad (k_8 \sim 1.5\times10^{-10}\ cm^3/s) \qquad (R8)$$

$$HBr + OH \rightarrow H_2O + Br \quad (k_9 \sim 8.0\times10^{-12}\ cm^3/s) \qquad (R9)$$

$$Br_2 + O \rightarrow BrO + Br \quad (k_{10} \sim 1.3\times10^{-11}\ cm^3/s) \qquad (R10)$$

$$Br_2 + O(^1D) \rightarrow BrO + Br \quad (k_{11} \sim 1.3\times10^{-10}\ cm^3/s) \qquad (R11)$$

$$Br_2 + OH \rightarrow HOBr + Br \quad (k_{12} \sim 3.1\times10^{-11}\ cm^3/s) \qquad (R12)$$

At the same time, the conditions $k_7[O] + k_9[OH] << k_1n_e$, $k_{10}[O] + k_{12}[OH] << k_2n_e$ and $[O(^1D)] << [O]$ imply that the efficiency of these channels is much lower compared with those of R1 and R2. In addition, each reaction inside the R10–R12 group liberates only one Br atom while the other one appears to be located in the BrO or HOBr molecule. All these suppress the total Br atom formation rate and result in a weak decrease in Br atom density compared with pure HBr plasma.

The substitution of HBr for Cl_2 in the HBr + Cl_2 + 11% O_2 gas mixture provides the decreasing rates of R1 and R2, but simultaneously introduces new formation pathways for Br atoms through R13: $HBr + Cl \rightarrow HCl + Br$ ($k_{13} \sim 2.0\times10^{-11}$ cm^3/s) and R14: $Br_2 + Cl \rightarrow Br + BrCl$ ($k_{14} \sim 1.5\times10^{-10}$ cm^3/s). Since the latter have quite high rate coefficients, the fast decay of HBr, and Br_2, as well as the rapidly increasing formation rates and densities for both HCl and BrCl are observed. Accordingly, reactions R15: $HCl + e \rightarrow H + Cl + e$ ($k_{15} \sim 1.2\times10^{-9}$ cm^3/s at T_e = 3 eV), R16: $BrCl + e \rightarrow Br + Cl + e$ ($k_{16} \sim 1.1\times10^{-8}$ cm^3/s at T_e = 3 eV) and R17: $BrCl + Cl \rightarrow Cl_2 + Br$ ($k_{17} \sim 1.5\times10^{-11}$ cm^3/s) also begin to be an essential source of Br atoms in the range of 20–81% Cl_2. Another important feature is that the rate coefficients for R7–R9 and R10–R12 are noticeably higher than those for R18–R20:

$$Cl_2 + O \rightarrow ClO + Cl \quad (k_{18} \sim 3.0\times10^{-13}\ cm^3/s) \qquad (R18)$$

$$Cl_2 + O(^1D) \rightarrow ClO + Cl \quad (k_{19} \sim 3.6\times10^{-11}\ cm^3/s) \qquad (R19)$$

$$Cl_2 + OH \rightarrow HOCl + Cl \quad (k_{20} \sim 4.0\times10^{-14}\ cm^3/s) \qquad (R20)$$

That is why an increase in y(Cl_2) sufficiently reduces the consumption rates for O, O(^{1}D) and OH species, provides the rapid increase in their densities (by ~ 2.7 times for O, ~ 5.2 times for O(^{1}D) and ~ 3.7 times for OH at 0-21% Cl_2, see Fig. 2) and accelerates the dissociation of both HBr and Br_2 through R7–R9 and R10–R12. All these effects, together with increasing electron impact dissociation frequencies for both HBr (k_1n_e = 2.0-9.7 s^{-1} for 0-89% Cl_2) and Br_2 (k_2n_e = 19-82 s^{-1} for 0-89% Cl_2), results in non-monotonic behavior for both the effective Br atom formation rate and [Br] value. The density of Cl atoms increase monotonically, but slower than expected from the linear change in y(Cl_2). This is due to the high Cl atom consumption rate through R13, R14 and R17 in HBr-rich plasmas.

The data on plasma parameters and densities of neutral species discusses above allows one to evaluate how the HBr/Cl_2 mixing ratio may influence the Si and SiO_2 etching kinetics. According to Refs. [17, 25], the rate of ion-assisted heterogeneous chemical reactions may be expressed as $R = \gamma_R\Gamma$, where Γ is the flux of chemically active neutral species, and γ_R is the effective reaction probability. From several published works, it can be understood that 1) the differences in the halogenation degrees for Si surfaces exposed to pure Cl_2 and HBr plasmas are in agreement with the differences in corresponding atom size [26]; 2) the differences in silicon etching rates in pure Cl_2 and HBr plasmas [27, 28] are in agreement with the differences in corresponding halogen atom and ion fluxes [7, 13, 16];

3) the Si etching yields pure Cl_2 and HBr plasmas at one and the same ion bombardment energy are very close [7]; and 4) the change in Si etching yield with variations of Cl_2/HBr mixing ratio at constant ion bombardment energy does not exceed the experimental error [7]. Therefore, one can suggest the effective reaction probabilities for Br and Cl atoms with Si surface being quite close. Probably, the same suggestion may be applied for SiO_2. As such, one can simply operate with the total chemical active flux $\Gamma_{Br} + \Gamma_{Cl}$ when analyzing the Si and SiO_2 etching kinetics. The parameter γ_R for ion-assisted chemical reaction is controlled by several ion-surface interaction pathways [25]. In the case of Si and SiO_2, these are: 1) the ion-stimulated desorption of reaction products, as the boiling points for both $SiCl_4$ (~ 58 °C) and $SiBr_4$ (~ 154 °C) [29] exceed the typical process temperature; and 2) the destruction of Si-O bonds, as the corresponding bond strength (~ 800 kJ/mol) is much higher for than for Si-Br (~ 358 kJ/mol) Si-Cl (~ 416 kJ/mol) [29]. The partial rate of each ion-driven pathway is $Y_S\Gamma_+$, where Y_S is the ion-type-averaged process yield. Since Y_S has a nature of sputtering yield, it is determined by the momentum transferred from the incident ion in a single collision [5]. Accordingly, the influence of HBr/Cl_2 mixing ratio on the kinetics of both ion-stimulated desorption of reaction products and Si-O bond breaking may be characterized by the parameter $(M_i\varepsilon_i)^{1/2}\Gamma_+$, where M_i is the effective ion molar mass.

From Fig. 3, it can be seen that the substitution of HBr for Cl_2 in the $HBr+Cl_2+O_2$ feed gas results in monotonically increasing $\Gamma_{Br} + \Gamma_{Cl}$ (6.4×10^{16}-1.2×10^{18} $cm^{-2}s^{-1}$ for 0-89% Cl_2). Also, thought decreases in both $-U_{dc}$ (404–351 V for 0-89% Cl_2) and ion bombardment energy (420-368 eV for 0-89% Cl_2) take place, this tendency is completely overcompensated by increasing ion flux ($\Gamma_+ = 2.9\times10^{15}$-$4.8\times10^{15}$ $cm^{-2}s^{-1}$ for 0-89% Cl_2). As such, the parameter $(M_i\varepsilon_i)^{1/2}\Gamma_+$ also exhibits an increase in the range 4.8×10^{17}-6.7×10^{17} $eV^{1/2}cm^{-2}s^{-1}$. Though the last fact evidently shows an increase in the ion bombardment efficiency, it does not mean directly the same effect on γ_R. One can imagine that the behavior γ_R in $HBr+Cl_2+O_2$ gas mixture is influenced by an additional factor connected with the chemistry of O atoms. The mechanisms responsible for the negative impact of O atoms on γ_R for both Si and SiO_2 may be connected with: 1) the formation of Si-O bonds that increases the reaction threshold for F atoms; and 2) the oxidation of reaction products into lower volatile $SiBr_xO_y$ and $SiCl_xO_y$ compounds. Obviously, the last mechanism decreases the desorption yield for reaction products and, thus, lowers the fraction of etched surfaces that are available for the adsorption of F atoms. Assuming that both ion energy flux and the O atoms flux have a nearly proportional, but opposite influences on γ_R, one can roughly characterize their competitive effect by the $\Gamma_O/(M_i\varepsilon_i)^{1/2}\Gamma_+$ ratio. Figure 3 shows that a change in $y(Cl_2)$ results in a much faster increase in Γ_O (1.1×10^{14}-1.2×10^{16} $cm^{-2}s^{-1}$, or by ~ 110 times for 0-89% Cl_2) compared with $(M_i\varepsilon_i)^{1/2}\Gamma_+$ and thus, provides a monotonically increasing $\Gamma_O/(M_i\varepsilon_i)^{1/2}\Gamma_+$ ratio toward Cl_2-rich plasmas. Therefore, a decrease in γ_R looks quite probable.

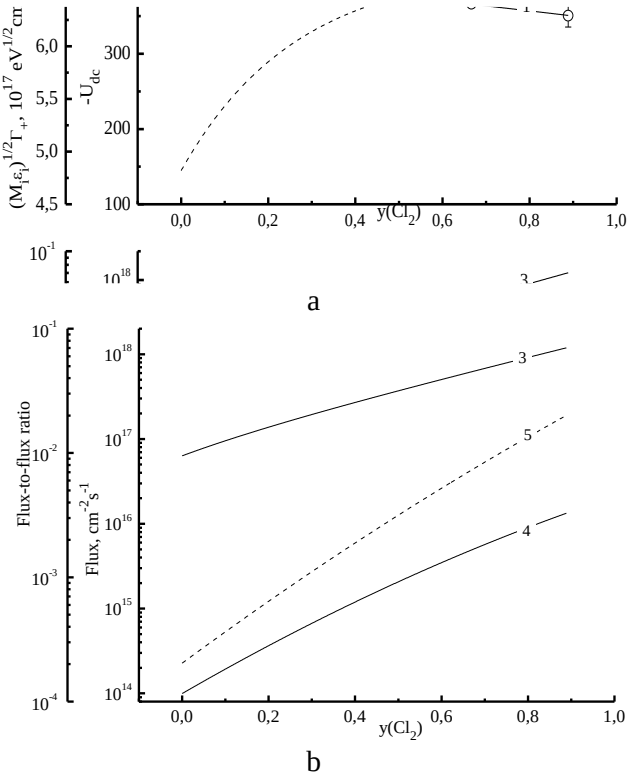

Fig. 3. Fluxes of active species and flux-to-flux ratios as functions of Cl_2 fraction in a feed gas. In Fig. a): 1–negative dc bias; 2–ion energy flux $(M_i\varepsilon_i)^{1/2}\Gamma_+$. In Fig. b): 3–total halogen atom flux; 4–oxygen atom flux; 5–$\Gamma_O/(M_i\varepsilon_i)^{1/2}\Gamma_+$ ratio. The process conditions correspond to Fig. 1

Рис. 3. Потоки активных частиц и отношения потоков в зависимости от содержания Cl_2 в исходной смеси. На рис. а): 1–отрицательное смещение на подложкодержателе; 2–поток энергии ионов $(M_i\varepsilon_i)^{1/2}\Gamma_+$. На рис. б): 3–суммарный поток атомов галогенов; 4–поток атомов кислорода; 5–отношение $\Gamma_O/(M_i\varepsilon_i)^{1/2}\Gamma_+$. Условия процесса соответствуют рис. 1

Summarizing above data, one can conclude that the change in HBr/Cl_2 mixing ratio (as well as in any other input parameter which exhibits the similar influence on formation/decay kinetics for plasma active species) may result in the competitive effect of increasing halogen atoms flux and decreasing effective reaction probability. Probably, such situation disturbs

well-known correlations between input process parameters and both Si and SiO_2 etching rates found for F-bases etching chemistries and thus, complicates the optimization of process regimes.

CONCLUSIONS

This work dealt with the effect of HBr/Cl_2 mixing ratio in HBr + Cl_2 + 11% O_2 gas mixture on gas-phase plasma characteristics under conditions of low-pressure inductive 13.56 MHz discharge. The investigation procedure combined plasma diagnostics by Langmuir probes and 0-dimensional (global) plasma modeling. It was found that the substitution of HBr for Cl_2: 1) results in increasing mean electron energy, electron density and total positive ion density; 2) causes the non-monotonic (with a maximum at ~ 45% Cl_2) change in Br atom density; and 3) provides the sufficient increase in O atom density. The net changes in gas-phase plasma characteristics may cause the competitive effect of increasing halogen atoms flux and decreasing effective reaction probabilities for both Si and SiO_2. The most realistic mechanism for the decrease in effective reaction probabilities toward Cl_2-rich plasmas is connected with the formation of low-volatile $SiBr_xO_y$ and $SiCl_xO_y$ product layers, which reduces the permittivity of halogen atoms and ions toward the etched surface.

The publication was carried out within the framework of the state assignment of the Federal State Institution FNC NIISI RAS (fundamental research) on subject No. 0065-2019-0006 "Fundamental and applied research in the field of sub wave holographic lithography, physical and chemical etching processes of 3D nanometer dielectric structures for the development of critical technologies for the production of ECB ".

REFERENCES
ЛИТЕРАТУРА

1. **Rooth J.R.** Industrial Plasma Engineering. Philadelphia: IOP Publishing LTD. 2001. 658 p.
2. Plasma Etching Processes for CMOS Devices Realization. London: ISTE Press–Elsevier. 2017. 125 p.
3. **Makabe T., Petrovic Z.** Plasma electronics: applications in microelectronic device fabrication. New York: Taylor & Francis. 2006. 330 p.
4. **Wolf S., Tauber R.N.** Silicon Processing for the VLSI Era. V. 1. Process Technology. New York: Lattice Press. 2000. 416 p.
5. **Lieberman M.A., Lichtenberg A.J.** Principles of plasma discharges and materials processing. New York: John Wiley & Sons Inc. 2005. 730 p. DOI: 10.1002/0471724254.
6. **Nojiri K.** Dry Etching Technology for Semiconductors. New York: Springer. 2015. 120 p. DOI: 10.1007/978-3-319-10295-5.
7. **Vitale S.A., Chae H., Sawin H.H.** Silicon etching yields in F_2, Cl_2, Br_2, and HBr high density plasmas. *J. Vac. Sci. Technol. A.* 2001. V. 19. N 5. P. 2197-2206. DOI: 10.1116/1.1378077.
8. **Cunge G., Kogelschatz M., Joubert O., Sadeghi N.** Plasma-wall interactions during silicon etching processes in high-density $HBr/Cl_2/O_2$ plasmas. *Plasma Sources Sci. Technol.* 2005. V. 14. N 2. P. S42-S52. DOI: 10.1088/0963-0252/14/2/S06.
9. **Kim D.K., Kim Y.K., Lee H.** A study of the role of HBr and oxygen on the etch selectivity and the post-etch profile in a polysilicon/oxide etch using HBr/O_2 based high density plasma for advanced DRAMs. *Mat. Sci. Semicon. Proc.* 2007. V. 10. N 1. P. 41-48. DOI: 10.1016/j.mssp.2006.08.027.
10. **Belen R.J., Gomez S., Kiehlbauch M., Aydil E.S.** Feature scale model of Si etching in $SF_6/O_2/HBr$ plasma and comparison with experiments. *J. Vacuum Sci. Technol. A.* 2006. V. 24. N 2. P. 350-361. DOI: 10.1116/1.2173268.
11. **Tinck S., Boullart W., Bogaerts A.** Modeling $Cl_2/O_2/Ar$ inductively coupled plasmas used for silicon etching: effects of SiO_2 chamber wall coating. *Plasma Sources Sci. Technol.* 2011. V. 20. P. 045012. DOI: 10.1088/0963-0252/20/4/045012.
12. **Yeom G. Y., Ono Y., Yamaguchi T.** Polysilicon etchback plasma process using HBr, Cl_2, and SF_6 gas-mixtures for deep-trench isolation. *J. Electrochem. Soc.* 1992. V. 139. N 2. P. 575-579. DOI: 10.1149/1.2069260.
13. **Efremov A., Lee J., Kwon K.H.** A comparative study of CF_4, Cl_2 and HBr + Ar inductively coupled plasmas for dry etching applications. *Thin Solid Films*. 2017. V. 629. P. 39-48. DOI: 10.1016/j.tsf.2017.03.035.
14. **Shun'ko E.V.** Langmuir probe in theory and practice. Boca Raton: Universal Publishers. 2008. 245 p.
15. **Caneses J.F., Blackwell B.** RF compensation of double Langmuir probes: modelling and experiment. *Plasma Sources Sci. Technol.* 2015. V. 24. P. 035024. DOI: 10.1088/0963-0252/24/3/035024.
16. **Efremov A., Kim Y., Lee H.W., Kwon K.H.** A comparative study of HBr-Ar and $HBr-Cl_2$ plasma chemistries for dry etch applications. *Plasma Chem. Plasma Proc.* 2011. V. 31. N 2. P. 259-271. DOI: 10.1007/s11090-010-9279-7.
17. **Efremov A.M., Kim D.P., Kim C.I.** Simple model for ion-assisted etching using Cl_2-Ar inductively coupled plasma: Effect of gas mixing ratio. *IEEE Trans. Plasma Sci.* 2004. V. 32. N 3. P. 1344-1351. DOI: 10.1109/TPS.2004.828413.
18. **Hsu C.C., Nierode M.A., Coburn J.W., Graves D.B.** Comparison of model and experiment for Ar, Ar/O_2 and $Ar/O_2/Cl_2$ inductively coupled plasmas. *J. Phys. D Appl. Phys.* 2006. V. 39. N 15. P. 3272-3284. DOI: 10.1088/0022-3727/39/15/009.
19. **Chistophorou L.G., Olthoff J.K.** Fundamental electron interactions with plasma processing gases. New York: Springer Science+Business Media. 2004. 780 p. DOI: 10.1007/978-1-4419-8971-0.
20. **Kwon K.H., Efremov A., Kim M., Min N.K., Jeong J., Kim K.** A model-based analysis of plasma parameters and composition in HBr/X (X=Ar, He, N_2) inductively coupled plasmas. *J. Electrochem Soc.* 2010. V. 157. N 5. P. H574-H579. DOI: 10.1149/1.3362943.
21. **Efremov A., Min N.K., Choi B.G., Baek K.H., Kwon K.H.** Model-based analysis of plasma parameters and active species kinetics in Cl_2/X (X = Ar, He, N_2) inductively coupled plasmas. *J. Electrochem. Soc.* 2008. V. 155. N 12. P. D777-D782. DOI: 10.1149/1.2993160.
22. **Lee B.J., Lee B.J., Efremov A., Yang J.W., Kwon K.H.** Etching characteristics and mechanisms of MoS_2 2D Crystals in O_2/Ar inductively coupled plasma. *J. Nanosci. Nanotechnol.* 2016. V. 16. N 11. P. 11201-11209. DOI: 10.1166/jnn.2016.13478.
23. **Kwon K.H., Efremov A., Yun S.J., Chun I., Kim K.** Dry etching characteristics of Mo and Al_2O_3 films in $O_2/Cl_2/Ar$ inductively coupled plasmas. *Thin Solid Films.* 2014. V. 552. P. 105-110. DOI: 10.1016/j.tsf.2013.12.013.

24. **Efremov A.M., Kim G.H., Kim J.G., Bogomolov A.V., Kim C.I.** On the applicability of self-consistent global model for the characterization of Cl_2/Ar inductively coupled plasma. *Microelectron. Eng.* 2007. V. 84. P.136-143. DOI: 10.1016/j.mee.2006.09.020.
25. **Gray D.C., Tepermeister I., Sawin H.H.** Phenomenological modeling of ion-enhanced surface kinetics in fluorine-based plasma-etching. *J. Vac. Sci. Technol. B.* 1993. V. 11. N 4. P. 1243-1257. DOI: 10.1116/1.586925.
26. **Cheng C.C., Guinn K.V., Herman I.P., Donnelly V.M.** Competitive halogenation of silicon surfaces in HBr/Cl_2 plasmas studied ray photoelectron-spectroscopy and in-situ, real-time, pulsed laser-induced thermal-desorption. *J. Vac. Sci. Technol. A.* 1995. V. 13. N 4. P. 1970-1976. DOI: 10.1116/1.579638.
27. **Bestwick T.D., Oehrlein G.S.** Reactive ion etching of silicon using bromine containing plasmas. *J. Vac. Sci. Technol. A.* 1990. V. 8. N 3. P. 1696-1701. DOI: 10.1116/1.576832.
28. **Jin W.D., Vitale S.A., Sawin H.H.** Plasma-surface kinetics and simulation of feature profile evolution in Cl_2+HBr etching of polysilicon. *J. Vac. Sci. Technol. A.* 2002. V. 20. N 6. P. 2106-2114. DOI: 10.1116/1.1517993.
29. **Lide D.R.** Handbook of chemistry and physics. New York: CRC Press. 2018. 1532 p.
30. **Guettari M., Gharbi A.** A correspondence between Grunberg–Nissan constant d′ and complex varieties in water/methanol mixture. *Phys. Chem. Liq.* 2011. V. 49. P. 459-469. DOI: 10.1080/00319101003646546.
31. **Herráez J.V., Belda R., Díez O., Herráez V.** An equation for the correlation of viscosities of binary mixtures. *J. Solution Chem.* 2008. V. 37. P. 233. DOI: 10.1007/s10953-007-9226-2.
32. **Marczak W., Adamczyk N., Łężniak M.** Viscosity of associated mixtures approximated by the Grunberg-Nissan model. *Int. J. Thermophys.* 2012. V. 33. P. 680-691. DOI: 10.1007/s10765-011-1100-1.
33. **Messaâdi A., Ouerfelli N., Das D., Hamda H., Hamzaoui A.H.** Correspondence between Grunberg–Nissan, Arrhenius and Jouyban–acree parameters for viscosity of isobutyric acid+water binary mixtures from 302.15 to 313.15 K. *J. Solution Chem.* 2012. V. 41. P. 2186-2208. DOI: 10.1007/s10953-012-9931-3.

Поступила в редакцию (Received) 21.12.2018
Принята к опубликованию (Accepted) 25.03.2019